HHS Public Access

Author manuscript

J Genet Genomics. Author manuscript; available in PMC 2015 December 21.

Published in final edited form as:

J Genet Genomics. 2015 June 20; 42(6): 319–330. doi:10.1016/j.jgg.2015.03.012.

Fast-Suppressor Screening for New Components in Protein Trafficking, Organelle Biogenesis and Silencing Pathway in *Arabidopsis thaliana* Using DEX-Inducible *FREE1-RNAi* Plants

Qiong Zhao[a], **Caiji Gao**[a], **PoShing Lee**[a], **Lin Liu**[b], **Shaofang Li**[b], **Tangjin Hu**[c], **Jinbo Shen**[a], **Shuying Pan**[c], **Hao Ye**[c], **Yunru Chen**[d], **Wenhan Cao**[a], **Yong Cui**[a], **Peng Zeng**[e], **Sheng Yu**[d], **Yangbin Gao**[f], **Liang Chen**[g], **Beixin Mo**[h], **Xin Liu**[e], **Shi Xiao**[g], **Yunde Zhao**[f], **Silin Zhong**[d], **Xuemei Chen**[b], and **Liwen Jiang**[a,c,*]

[a]Centre for Cell & Developmental Biology and State Key Laboratory of Agrobiotechnology, School of Life Sciences, The Chinese University of Hong Kong, Shatin, New Territories, Hong Kong, China

[b]Department of Botany and Plant Sciences, Institute of Integrative Genome Biology, University of California, Riverside, CA 92521, USA

[c]CUHK Shenzhen Research Institute, The Chinese University of Hong Kong, Shenzhen 518057, China

[d]School of Life Sciences, The Chinese University of Hong Kong, Shatin, New Territories, Hong Kong, China

[e]Beijing Genomics Institute at Shenzhen, Shenzhen 518083, China

[f]Section of Cell and Developmental Biology, University of California San Diego, La Jolla, CA 92093, USA

[g]State Key Laboratory of Biocontrol and Guangdong Key Laboratory of Plant Resources, School of Life Sciences, Sun Yat-sen University, Guangzhou 510275, China

[h]Shenzhen Key Laboratory of Microbial Genetic Engineering, College of Life Sciences, Shenzhen University, Shenzhen 518060, China

Abstract

Membrane trafficking is essential for plant growth and responses to external signals. The plant unique FYVE domain-containing protein FREE1 is a component of the ESCRT complex (endosomal sorting complex required for transport). FREE1 plays multiple roles in regulating protein trafficking and organelle biogenesis including the formation of intraluminal vesicles of multivesicular body (MVB), vacuolar protein transport and vacuole biogenesis, and autophagic degradation. FREE1 knockout plants show defective MVB formation, abnormal vacuolar transport, fragmented vacuoles, accumulated autophagosomes, and seedling lethality. To further uncover the underlying mechanisms of FREE1 function in plants, we performed a forward genetic

*Corresponding author. Tel: +852 3943 6388, fax: +852 3943 5646. ljiang@cuhk.edu.hk. .

SUPPLEMENTARY DATA

Supplementary data related to this article can be found at http://dx.doi.org/10.1016/j.jgg.2015.03.012.

screen for mutants that suppressed the seedling lethal phenotype of *FREE1-RNAi* transgenic plants. The obtained mutants are termed as suppressors of *free1* (*sof*). To date, 229 putative *sof* mutants have been identified. Barely detecting of FREE1 protein with M_3 plants further identified 84 FREE1-related suppressors. Also 145 mutants showing no reduction of FREE1 protein were termed as RNAi-related mutants. Through next-generation sequencing (NGS) of bulked DNA from F_2 mapping population of two RNAi-related *sof* mutants, *FREE1-RNAi* T-DNA inserted on chromosome 1 was identified and the causal mutation of putative *sof* mutant is being identified similarly. These FREE1- and RNAi-related *sof* mutants will be useful tools and resources for illustrating the underlying mechanisms of FREE1 function in intracellular trafficking and organelle biogenesis, as well as for uncovering the new components involved in the regulation of silencing pathways in plants.

Keywords

Suppressors; FREE1; Endomembrane trafficking; *Arabidopsis*; NGS

INTRODUCTION

The plant endomembrane system contains several functionally distinct membrane-bound organelles including endoplasmic reticulum (ER), golgi apparatus, trans-golgi network (TGN) or early endosome, prevacuolar compartment (PVC) or multivesicular body (MVB) or late endosome, and vacuoles (Lam et al., 2007; Reyes et al., 2011; Gao et al., 2014a). Membrane trafficking within the endomembrane system is essential for protein and lipid material transport and exchange within and in-between cells. In plants, the trafficking system functions for both fundamental cellular activities and also responds to environmental stresses (Samaj et al., 2006; Bar and Avni, 2014; Teh and Hofius, 2014).

Plant cells have highly regulated membrane trafficking pathways that are conserved among eukaryotic cells, but also seem to have evolved additional features with some of the components present in multiple copies (Cvrckova et al., 2012). The plant endomembrane machinery was largely established from homology-based studies (Bassham et al., 2008). For example, the endosomal sorting somplex required for transport (ESCRT) machinery regulates the homeostasis of plasma membrane protein by sorting them into the MVB which eventually fuse with the lytic vacuole to degrade the ubiquitinated plasma membrane (PM) cargo molecules (Henne et al., 2011; Cai et al., 2014). Most of our current knowledge on ESCRT in plants comes mainly by homology with studies performed on yeast and humans. However, orthologs of the subunits of ESCRT-0 have not been identified in plants (Leung et al., 2008).

A recent study of the plant unique FYVE domain containing protein FREE1 (FYVE domain protein required for endosomal sorting 1) showed that FREE1 localizes to the PVC, and interacts with the ESCRT-I component Vps23 to regulate the formation of intraluminal vesicles (ILVs) in PVCs/MVBs thereby facilitating PM protein degradation in the vacuole (Gao et al., 2014b). Mutant plants without functional FREE1 (T-DNA and RNAi mutants) are seedling lethal, defective in MVB ILV biogenesis and vacuolar sorting of membrane

proteins. They also show abnormalities in vacuolar trafficking and accumulate small fragmented vacuoles and autophagosomes (Gao et al., 2014b, 2015). FREE1 was found to directly interact with SH3P2, a unique regulator of plant autophagy (Zhuang et al., 2013; Zhuang and Jiang 2014), thus controlling autophagosome-vacuole fusion and finally autophagic degradation in plants (Gao et al., 2015). These studies have unveiled a direct link between the ESCRT machinery and autophagy process, and demonstrate the multiple functional roles of FREE1 in regulating MVB formation, vacuolar protein transport, vacuole biogenesis and autophagy pathway. Because of the multiple functions of FREE1 in *Arabidopsis*, it is likely that plants have evolved unique mechanisms and components responsible for the FREE1-containing ESCRT pathway. It is now clear that FREE1 has dual roles in regulating membrane trafficking: 1) through FREE1 N-terminal direct interaction with ESCRT1 components VPS23, FREE1 regulates MVB biogenesis and PM protein vacuolar degradation; 2) through FREE1 C-terminal direct interaction with the autophagosome regulator SH3P2 (Zhuang et al., 2013; Zhuang and Jiang 2014), FREE1 regulates autophagosome formation and autophagic degradation (Gao et al., 2015). In addition, the abnormalities in *free1* mutant including the dysfunction of vacuolar protein transport and autophagic degradation point to a defect in membrane fusion caused by FREE1 depletion. However, it is still not understood why and how FREE1 depleted cells contain fragmented small vacuoles and how FREE1 loss-of-function leads to seedling death. It is likely that the functions of proteins required for docking and/or fusion with vacuoles might be disrupted in the *free1* mutant. Alternatively, FREE1 might work together with other proteins to regulate membrane fusion and vacuole biogenesis through as yet undefined mechanisms.

To address how FREE1 fulfills its multiple roles in regulating membrane trafficking and organelle biogenesis in plants, we performed a suppressor screen using a FREE1 loss-of-function mutant as the starting material. With the emerging technology of next-generation sequencing (NGS), the mutated gene can be identified through an NGS-mapping approach in a short time (Manavella et al., 2012). Here, we report on the NGS-based high-throughput suppressor identification method to find mutants that can rescue the *free1* seedling lethal phenotype using inducible *FREE1-RNAi* plants. Upon dexamethasone (DEX) induction, the *FREE1-RNAi* transgenic plants are seedling lethal with the FREE1 protein barely detectable. Seeds from *FREE1-RNAi* plants were treated with EMS for suppressor screening. M_2 seeds were sprayed on plates with DEX to identify surviving plants, which we name *sof* (suppressors of *free1*. Because some of the isolated mutants could be caused by a disruption of the RNAi process, we also performed a second screen through Western blot analysis using FREE1 antibodies. We selected mutants with significantly reduced FREE1 proteins as putative *sof* mutants (termed as FREE1-related *sof* mutants) for further characterization. Using this method, we have successfully isolated 84 FREE1-related *sof* mutants. These SOF probably encode proteins involved in controlling vacuole biogenesis and vacuolar trafficking. All of these FREE1-related *sof* mutants and RNAi-related mutants will be useful resources for members of the international research community working on novel mechanisms of regulating organelle and RNA biogenesis in plants.

RESULTS

Establishment of the mutant pool and screening process

Using the Columbia ecotype (Col) as the wild type, *FREE1-RNAi* M_0 seeds were successfully generated with the wild type transformed with *pTA7002* construct containing the hairpin *FREE1-RNAi* (Fig. 1A). T_3 seeds from individual hygromycin resistant T_2 lines were screened on both DEX and hygromycin conditions. Line 11# was chosen as mutagenesis material because 3/4 of its T_3 showed hygromycin resistance and lethal phenotype on DEX, supporting the single copy insertion of *pTA7002-FREE1-RNAi*. Homozygous Line 11# was used for following EMS treatment and RNA and protein analysis. The successful induction of the FREE1 silencing system in *FREE1-RNAi* line was confirmed by RNA blot analysis with significant FREE1-siRNA accumulation and by Western blot analysis with little detection of FREE1 (Fig. 1B and C), and the silencing of FREE1 resulted in seedling lethality (Fig. 1D). For *sof* mutant screening, M_2 seeds were planted on MS plates supplied with 10 μmol/L DEX, and surviving plants were selected (Fig. 1E and F).

Identification of *sof* mutants

To confirm whether the screened M_2 mutations were heritable, M_3 seeds collected from individual M_2 plants were screened on MS plates with 10 μmol/L DEX. Seedlings that showed recovered phenotype similar to the wild type (as those in Fig. 2A) were further analyzed as putative *sof* mutants. To classify whether the putative *sof* mutants were FREE1-related or RNAi related, FREE1 protein levels were determined by Western blot using cFBPase as the loading control. As summarized in Table 1, we screened out 84 FREE1-related and 145 RNAi-related *sof* mutants. The 84 candidates showed reduced expressions of FREE1 including *sof220* and *sof641* in Fig. 2B, which were categorized into the FREE1-related mutants (Table S1); 145 candidates (Table S2) showed an unchanged FREE1 protein level including *sof18* and *sof30*, which were grouped as the RNAi-related mutants. Representatives of both types of mutants with altered phenotypes are shown in Figs. S1 and S2, respectively.

Fragmented vacuole morphology is restored in FREE1-related *sof* mutants

To test whether FREE1-related *sof* mutants were able to restore the fragmented vacuole phenotype of *FREE1-RNAi* plants, FM4-64 dye staining was performed to reflect the vacuole morphology. As shown in Fig. 3, upon DEX induction, the *FREE1-RNAi* plants showed numerous fragmented vacuoles (as indicated by arrows) while the wild type had a central large vacuole. It is possible that down-regulation of endogenous FREE1 may affect cell division or cell shape in the cotyledon epidermal cells compared to the wild-type cells. However, in the two FREE1-related *sof* mutants *sof220* and *sof641*, vacuole morphology may have been restored to a large central vacuole. Similar patterns were observed in other FREE1-related candidates. Rapid DAPI staining was also applied for visualizing the cell shape (Spitzer et al., 2009).

NGS-mapping workflow

To identify the mutated *SOF* gene, an outcross-mapping population was established by crossing *sof* mutants to Landsberg erecta (Ler) wild type. The genome (representing all chromosomes) of Ler is marked in red and Col is marked in blue (Fig. 4A). Based on genetic analysis, *FREE1-RNAi* transgenic plants are confirmed to harbor a single-insertion (as indicated by R in blue, representing its insertion in certain chromosome). All *sof* mutants are assumed to harbor a mutation (as indicated by m in green, representing the possible location in any chromosomes) caused by EMS. The putative mutants were crossed with Ler and marked as F_1 seeds, and F_1 selfing generates F_2 populations (Fig. 4B). The F_2 seeds were screened on MS plates supplemented with DEX and Hyg. The F_2 seeds with small scale (~100 seeds) were first analyzed to see whether that 3/16 of total seedlings was able to survive (for detailed genetic analysis, see Tables S3 and S4). With a 3/16 segregation ratio, we screened the F_2 in large scale use a more strict selection to reduce the mis-scored individuals, then more than 250 seedlings showing a convincing surviving phenotype were selected from more than 2500 F_2 seeds. The genomic DNA was used for library preparation and DNA sequencing (Fig. 4C and D).

NGS-mapping analysis strategy and simulated results

Instead of using traditional PCR-based mapping methods, we used NGS-mapping methods for gene identification. As shown in Fig. 5A, it is clear that the m site (*sof* suppressor mutation site) was enriched during the sample pooling process, and close to the m site, there will be an over-representation of Col background. Parental genotypes Col and Ler are known, then mapping-by-sequencing can be carried out on the basis of allele frequency estimations (AFE). The mutant AFE was calculated as the percentage of alleles from Col divided by all alleles aligned to the respective chromosome region (both Col and Ler). The Col allele frequency peak should correspond to the causal mutation m site. When the simulated reads (Fig. 5B and C) were plotted, the significant peak representing the enriched m site appeared (Fig. 5D). The fine mapping interval resides within the peak region that showed a high Col allele frequency, and the causal mutation will be identified within the peak regions.

Comparing to the recessive m site, other sites that unlinked with m site should mostly show a Col allele frequency of around 0.5 due to recombination events. However, the dominant R site (*FREE1-RNAi* T-DNA insertion site) is a little different among all sites unlinked with m site. As illustrated before (Fig. 4C), theoretically the selected F_2 should contain mutants that are homozygous at m site (all), homozygous at R site (1/3) and heterozygous mutants at R site (2/3), which means probably there is a mild peak corresponding to the R site (Fig. 5C and D).

Sequencing results of two *sof* mutants

As proof-of-principle, two RNAi-related *sof* mutants *sof18* and *sof30* were outcrossed to Ler, and the F_2 seeds were selected and sequenced following the previously described workflow (Fig. 4 and Table S4). With the whole-genome sequencing sample, the NGS-Mapping were carried out based on 461,070 SNP markers (Galvao et al., 2012). As expected, a peak specific to *sof18* was found located on the far right arm of chromosome 1

(Fig. S3), while the *sof30* specific peak located to chromosome 5 (Fig. S4). For each mutant, the fine mapping identified the candidate genes (with none of them published before) bearing meaningful mutations caused by EMS. As to these two novel mutants, further characterizations are in need to illustrate how they are involved in interrupting the FREE1-RNAi process. Meanwhile, for both *sof18* and *sof30*, shared peaks appeared on the left arm of chromosome 1, which indicates the R site of *FREE1-RNAi* T-DNA (Fig. 6A and B).

Identification of the *FREE1-RNAi* T-DNA insertion site by chimeric reads from whole genome sequencing

To confirm that the shared peaks correspond to the R site, we identified the chimeric reads containing sequence of both *FREE1-RNAi* T-DNA and Col genomic DNA from NGS data of *sof30*. Chimeric reads alignment to genome found that the chimeric reads located on chromosome 1 at position 8,303,184, which supports the expected R site at this shared peak region (Fig. 6C). The PCR amplified product was further subjected to Sanger sequencing using flanking primers LB and RP, and verified the *FREE1-RNAi* T-DNA insertion site at position 8,303,184 (Fig. 6D).

DISCUSSION

The significance of FREE1-related *sof* mutants

In *Arabidopsis*, forward genetic screening has identified mutants in development and signaling transduction pathways, and has also been applied to membrane trafficking studies (Page and Grossniklaus, 2002). For example, BEN1 was identified through screening for mutants with defects in constitutive endocytosis of the PIN1 auxin transporter (Tanaka et al., 2009). As always, enhancer and suppressor screening is helpful in discovering important players in the same pathway. For example, the identification of NPY1 as *yuc1yuc4* enhancer defined its critical role in auxin pathway (Cheng et al., 2007); the identification of the E3 ligase SP1 as suppressor of the *Arabidopsis* plastid protein import mutation *ppi1* led to the discovery of the ubiquitin-proteasome system in regulation of plastid development (Ling et al., 2012). However, it is hard to apply suppressor screening to lethal mutant plants. Here by using inducible *FREE1-RNAi* plants, we carried out a suppressor screening to identify new components involved in FREE1-mediated membrane trafficking pathways.

As summarized in Fig. 7, based on the FREE1 protein levels after DEX induction, putative *sof* mutants were categorized into FREE1-related and RNAi-related groups. Confirmed mutants were backcrossed with *FREE1-RNAi* to ascertain whether it was a single recessive or dominant mutation (Table S3), and outcrossed with Ler for gene identification (Table S4). For FREE1-related *sof* mutants, a cross with *free1* (T-DNA heterozygous mutants) mutants further verified the rescue of *free1* by certain *sof* mutants (Table S5). For screening of FREE1-related *sof* mutants *via* Western blot, we also screened out the mutants that were disrupted in the FREE1-RNAi process as we named RNAi-related *sof* mutants. To these mutants, detection of *FREE1-siRNA* with DEX will classify them into two groups, one group with no *FREE1-siRNA* detected while the other group showed no defects in *FREE1-siRNA* production. Further identification of these mutants will surely extend our current

knowledge about silencing pathways including transgene suppression, siRNA biogenesis and post-transcriptional gene silencing.

Successful isolation of the salt-tolerance mutant *sltA* in *Aspergillus nidulans* for the rescue of null mutations in ESCRT-0, I, II and III genes has linked sodium homeostasis with the ESCRT pathway, although the mechanism remains unclear (Calcagno-Pizarelli et al., 2011). As *Arabidopsis* lacks an *SLTA* ortholog, it is significant to identify new plant-specific components to help us in understanding the mechanisms for the roles of *FREE1* in the plant ESCRT machinery and also in the biogenesis of MVBs. At the whole plant level, we expect to understand the reasons why *FREE1* deficient plants are lethal through further studies on the newly identified genes. This will surely allow us to have a better understanding of the role of *FREE1* mediated membrane trafficking in early seedling development.

The advantages and problems of this suppressor screen

The severe DEX-inducible lethal phenotype of the *FREE1-RNAi* seedling provides an excellent basis to genetically dissect the FREE1-mediated membrane trafficking pathway through suppressor screening. Accordingly, we screened the ethyl methanesulfonate (EMS) mutagenized inducible *FREE1-RNAi* plants for suppressors.

The advantages of using inducible *FREE1-RNAi* plants include the followings: 1) Since the lethality caused by *FREE1-RNAi* is dominant, outcrosses of these candidate mutants into the Ler wild-type have allowed us to collect true mutants for gene identification (Table S2); 2) Since the lethal phenotype is inducible, crosses of putative FREE1-related *sof* mutants with *free1* T-DNA insertion mutants have enabled us to identify true *sof* suppressors in *FREE1* knock out mutants (Table S5); 3) We have used next-generation sequencing technology to facilitate the identification of the causal gene(s) in a timesaving and reliable manner.

On the other hand, the screening had the following problems. First, the classification of FREE1-related and RNAi-related mutants was mainly based on FREE1 protein detection with DEX. In our experience, it is hard to differentiate RNAi-related mutants from FREE1-related mutants when the reduction of *FREE1* was not significant. Second, some of the *sof* mutants were not able to reach a flowering stage, making it difficult to identify the gene.

Future work

Our on-going and future work will mainly focus on gene identification and a functional analysis of the putative FREE1-related *sof* mutants as well as some interesting RNAi-related *sof* mutants. These mutants are currently being processed for gene identification. Characterizing these mutants will help us gain valuable insights into how *FREE1* functions in coordinating normal membrane trafficking pathways and organelle biogenesis in relation to plant growth and development.

In addition, the application of this fast suppressor mutant screening approach can also be applied to other mutants involved in membrane trafficking and organelle biogenesis in plants. Indeed, we have recently extended such approach to screen for the *mon1 repressor* mutants for new components in regulating vacuole biogenesis (Cui et al., 2014); and suppressor screening using SH3P2-RNAi line for new modules in the autophagic pathway

(Zhuang et al., 2013; Zhuang and Jiang 2014); as well as suppressor screening using EXPO- or exocyst-related mutants for the EXPO-mediated unconventional protein secretion pathways in plants (Wang et al., 2010; Ding et al., 2012, 2014a, 2014b).

MATERIALS AND METHODS

Plant materials and growth conditions

Arabidopsis wild type (Col) plants were transformed with a *pTA7002* construct (Aoyama and Chua, 1997) harboring a hairpin *FREE1-RNAi* cassette (Wesley et al., 2001), and hygromycin resistant single insertion *FREE1-RNAi* transgenic plants were used for mutagenesis. The previously described *free1* mutant was designated *free1-1* (Gao et al., 2014b). Seeds were surface sterilized and grown on plates with full Murashige and Skoog (MS) salts (pH adjusted to 5.7 with 0.1 mol/L KOH) plus 3% sucrose and 0.8% agar at 22°C under a long-day (16 h light/8 h dark) photoperiod. For induction of *FREE1 RNAi*, 10 μmol/L DEX (10 mmol/L stock dissolved in ethanol) was added in the medium.

Mutants pool establishment

The mutant pool was established following a previous report with mild modification (An et al., 2010, Zhang et al., 2015). About 10,000 high quality seeds from single insertion *FREE1-RNAi* transgenic plants were soaked at 4°C in 40 mL dH_2O for 60 h, and then washed twice with 50 mL dH_2O. Washed seeds were treated with 0.3% EMS for 8 h with gentle shaking (~140 r/min) at room temperature. The seeds were then washed ten times with dH_2O (50 mL × 10). M_1 seeds were sprayed into 20 large square ports. For M_2 seeds collection, M_1 plants were divided into 283 subfamilies.

Phenotype screening for mutant isolation

M_2 seeds were surface-sterilized and sprayed on MS medium plus with 10 μmol/L DEX. Plates were kept at 4°C in dark for two days before placing in growth chambers. 5-day-old seedlings were screened for survived phenotypes. Selected M_2 seedlings were planted into soil for individual M_3 seeds collection. Individual M_3 seeds were screened on MS medium plus with 10 μmol/L DEX and hygromycin, and 5-day-old seedlings M_3 seedlings were screened for survived phenotype.

Protein extraction and Western blot analysis

For total protein extraction from plants, whole seedlings tissues were ground in liquid nitrogen and extracted with a lysis buffer containing 25 mmol/L Tris-HCl pH 7.5, 150 mmol/L NaCl, 1 mmol/L EDTA, 1 × Complete Protease Inhibitor Cocktail (Roche, USA) and 1% Triton X-100. The protein blot was hybridized with rabbit FREE1 antibodies (Gao et al., 2014b) and rabbit cFBPase antibodies (Agrisera, Cat No. AS04 043, SWEDEN).

FM-DYE staining and confocal microscopy analysis

FM-DYE staining was performed as described (Lam et al., 2008). Stock solutions of FM4-64 (12 mmol/L in DMSO; Invitrogen, USA) were prepared and stored at −20°C. Seedlings were first washed with MS liquid medium and stained for 3 h with FM4-64 which

was diluted to working solution at 12 μmol/L with MS liquid medium just before use. After staining, the seedlings were washed twice with fresh medium before confocal imaging. Rapid DAPI staining was carried as described (Spitzer et al., 2009). Images were collected using a 63 × objective water lens in the Leica SP8 Confocal system.

RNA extraction and RNA Northern blot

RNA isolation and northern blotting detection of *FREE1-siRNAs* were performed following a standard protocol as previously described (Park et al., 2002, Li et al., 2013). In brief, total RNAs of 10-day light-grown seedlings from DEX and MS conditions were extracted using TRIzol reagent. Probes against FREE1 siRNAs were labeled using 5′-end-labeling (32P) to detect siRNAs from total RNAs.

DNA extraction, library preparation and Illumina sequencing

Genomic DNA was prepared using DNeasy Plant Mini Kit (Qiagen, Cat No. 69104, USA) following the manufacturer's instruction. These sheared DNAs were sequentially ligated with the 3′ and 5′ adapters using the DNA library Preparation Kit (Illumina, USA) according to the manufacturer's instructions. The libraries were barcoded and sequenced on an Illumina Hiseq2000. The whole sequencing process was carried out following previous reported procedures (Zhong et al., 2013).

Sequence data analysis

For reference genome, the Col-0 (TAIR10) sequence was used. Both *sof18* and *sof30* are in Col background. Sequencing reads of *sof18* and *sof30* were aligned against the reference genome sequence (TAIR10) using SOAP2 (http://soap.genomics.org.cn/soapaligner.html), and consensus was called using SAM-TOOLS program (Li et al., 2009). NGS-Mapping was carried out based on 461,070 SNP markers using SHOREmap outcross function (Schneeberger et al., 2009; Galvao et al., 2012). Relatively reliable loci were filtered as below: consensus quality >20 (error rate, 1%), total depth >5. Only EMS induced C/G to T/A SNP markers were further considered as candidates.

Identification of the *FREE1-RNAi* T-DNA insertion site from whole genome sequencing

The site of the *FREE1-RNAi* T-DNA insertion was determined using the genome sequencing data from the bulk F_2 mapping population of *sof30*. The strategy was to identify chimeric reads with both T-DNA and genome DNA sequences. The reads from the *sof30* population were mapped to the *Arabidopsis* genome using BWA (Li and Durbin 2009) without mismatches. The unmapped reads were mapped back to the T-DNA insertion sequence using Blast (Zhang and Madden 1997). The reads containing perfect matches to the T-DNA sequence longer than 25 nt and shorter than 76 nt were retained. The unmapped parts of the retained reads were obtained and remapped to the *Arabidopsis* genome. In this way, the reads containing partial matches to the *Arabidopsis* genome were obtained, which are chimeric reads containing both T-DNA and flanking genomic DNA sequences.

Sequencing of *FREE1-RNAi* T-DNA insertion site

Primers (LP_5′-GCTTCTCGAAACCCATTTCATC-3′ and RP_5′-GAGCTTCAGGCTTCATAGGT-3′) flanking the T-DNA insertion site were used to amplify wild type fragment. Primers (LB_5′-ATTTCGGAACCACCATCAAACAG-3′ and RP_5′-GAGCTTCAGGCTTCATAGGT-3′) were used to amplify the mosaic fragment. The mosaic fragment was sequenced using standard Sanger sequencing methods.

Supplementary Material

Refer to Web version on PubMed Central for supplementary material.

ACKNOWLEDGMENTS

This work was supported by grants from the NIH GM114660 to Y. Zhao, the Research Grants Council of Hong Kong (CUHK466011, 465112, 466613, CUHK2/CRF/11G, C4011-14R and AoE/M-05/12), NSFC/RGC (N_CUHK406/12), NSFC (31270226 and 31470294), and Shenzhen Peacock Project (KQTD201101) to L. Jiang.

Abbreviations

AFE	allele frequency estimation
DEX	dexamethasone
ESCRT	endosomal sorting complex required for transport
FREE1	FYVE domain protein required for endosomal sorting 1
MVB	multivesicular body
NGS	next generation sequencing
sof	suppressor of *free1*

REFERENCES

An F, Zhao Q, Ji Y, Li W, Jiang Z, Yu X, Zhang C, Han Y, He W, Liu Y, Zhang S, Ecker JR, Guo H. Ethylene-induced stabilization of ETHYLENE INSENSITIVE3 and EIN3-LIKE1 is mediated by proteasomal degradation of EIN3 binding F-box 1 and 2 that requires EIN2 in *Arabidopsis*. Plant Cell. 2010; 22:2384–2401. [PubMed: 20647342]

Aoyama T, Chua NH. A glucocorticoid-mediated transcriptional induction system in transgenic plants. Plant J. 1997; 11:605–612. [PubMed: 9107046]

Bar M, Avni A. Endosomal trafficking and signaling in plant defense responses. Curr. Opin. Plant Biol. 2014; 22:86–92. [PubMed: 25282589]

Bassham DC, Brandizzi F, Otegui MS, Sanderfoot AA. The secretory system of *Arabidopsis*. Arabidopsis Book. 2008; 6:e0116. [PubMed: 22303241]

Cai Y, Zhuang XH, Gao CJ, Wang XF, Jiang LW. The *Arabidopsis* endosomal sorting complex required for transport III regulates internal vesicle formation of the prevacuolar compartment and is required for plant development. Plant Physiol. 2014; 165:1328–1343. [PubMed: 24812106]

Calcagno-Pizarelli AM, Hervas-Aguilar A, Galindo A, Abenza JF, Penalva MA, Arst HN Jr. Rescue of *Aspergillus nidulans* severely debilitating null mutations in ESCRT-0, I, II and III genes by inactivation of a salt-tolerance pathway allows examination of ESCRT gene roles in pH signalling. J. Cell Sci. 2011; 124:4064–4076. [PubMed: 22135362]

Cheng Y, Qin G, Dai X, Zhao Y. NPY1, a BTB-NPH3-like protein, plays a critical role in auxin-regulated organogenesis in *Arabidopsis*. Proc. Natl. Acad. Sci. USA. 2007; 104:18825–18829. [PubMed: 18000043]

Cui Y, Zhao Q, Gao C, Ding Y, Zeng Y, Ueda T, Nakano A, Jiang L. Activation of the Rab7 GTPase by the MON1-CCZ1 complex is essential for PVC-to-vacuole trafficking and plant growth in *Arabidopsis*. Plant Cell. 2014; 26:2080–2097. [PubMed: 24824487]

Cvrckova F, Grunt M, Bezvoda R, Hala M, Kulich I, Rawat A, Zarsky V. Evolution of the land plant exocyst complexes. Front. Plant Sci. 2012; 3:159. [PubMed: 22826714]

Ding Y, Wang J, Wang JQ, Stierhof YD, Robinson DG, Jiang LW. Unconventional protein secretion. Trends Plant Sci. 2012; 17:606–615. [PubMed: 22784825]

Ding Y, Wang J, Lai JHC, Chan VHL, Wang XF, Cai Y, Tan XY, Bao YQ, Xia J, Robinson DG, Jiang LW. Exo70E2 is essential for exocyst subunit recruitment and EXPO formation in both plants and animals. Mol. Biol. Cell. 2014a; 25:412–426. [PubMed: 24307681]

Ding Y, Robinson DG, Jiang L. Unconventional protein secretion (UPS) pathways in plants. Curr. Opin. Cell Biol. 2014b; 29:107–115. [PubMed: 24949560]

Galvao VC, Nordstrom KJ, Lanz C, Sulz P, Mathieu J, Pose D, Schmid M, Weigel D, Schneeberger K. Synteny-based mapping-by-sequencing enabled by targeted enrichment. Plant J. 2012; 71:517–526. [PubMed: 22409706]

Gao C, Cai Y, Wang Y, Kang BH, Aniento F, Robinson DG, Jiang L. Retention mechanisms for ER and Golgi membrane proteins. Trends Plant Sci. 2014a; 19:508–515. [PubMed: 24794130]

Gao C, Luo M, Zhao Q, Yang R, Cui Y, Zeng Y, Xia J, Jiang L. A unique plant ESCRT component, FREE1, regulates multivesicular body protein sorting and plant growth. Curr. Biol. 2014b; 24:2556–2563. [PubMed: 25438943]

Gao C, Zhuang X, Cui Y, Fu X, He Y, Zhao Q, Zeng Y, Shen J, Luo M, Jiang L. Dual roles of an *Arabidopsis* ESCRT component FREE1 in regulating vacuolar protein transport and autophagic degradation. Proc. Natl. Acad. Sci. USA. 2015; 112:1886–1891. [PubMed: 25624505]

Henne WM, Buchkovich NJ, Emr SD. The ESCRT pathway. Dev. Cell. 2011; 21:77–91. [PubMed: 21763610]

Lam SK, Tse YC, Robinson DG, Jiang L. Tracking down the elusive early endosome. Trends Plant Sci. 2007; 12:497–505. [PubMed: 17920331]

Lam SK, Cai Y, Hillmer S, Robinson DG, Jiang L. SCAMPs highlight the developing cell plate during cytokinesis in tobacco BY-2 cells. Plant Physiol. 2008; 147:1637–1645. [PubMed: 18508957]

Leung KF, Dacks 25 JB, Field MC. Evolution of the multivesicular body ESCRT machinery; retention across the eukaryotic lineage. Traffic. 2008; 9:1698–1716. [PubMed: 18637903]

Li H, Durbin R. Fast and accurate short read alignment with Burrows-Wheeler transform. Bioinformatics. 2009; 25:1754–1760. [PubMed: 19451168]

Li H, Handsaker B, Wysoker A, Fennell T, Ruan J, Homer N, Marth G, Abecasis G, Durbin R, Genome Project Data Processing, S. The Sequence Alignment/Map format and SAM tools. Bioinformatics. 2009; 25:2078–2079. [PubMed: 19505943]

Li S, Liu L, Zhuang X, Yu Y, Liu X, Cui X, Ji L, Pan Z, Cao X, Mo B, Zhang F, Raikhel N, Jiang L, Chen X. MicroRNAs inhibit the translation of target mRNAs on the endoplasmic reticulum in *Arabidopsis*. Cell. 2013; 153:562–574. [PubMed: 23622241]

Ling QH, Huang WH, Baldwin A, Jarvis P. Chloroplast biogenesis is regulated by direct action of the ubiquitin-proteasome system. Science. 2012; 338:655–659. [PubMed: 23118188]

Manavella PA, Hagmann J, Ott F, Laubinger S, Franz M, Macek B, Weigel D. Fast-forward genetics identifies plant CPL phosphatases as regulators of miRNA processing factor HYL1. Cell. 2012; 151:859–870. [PubMed: 23141542]

Page DR, Grossniklaus U. The art and design of genetic screens: *Arabidopsis thaliana*. Nature. 2002; 3:124–136.

Park W, Li J, Song R, Messing J, Chen X. CARPEL FACTORY, a Dicer homolog, and HEN1, a novel protein, act in microRNA metabolism in *Arabidopsis thaliana*. Curr. Biol. 2002; 12:1484–1495. [PubMed: 12225663]

Reyes FC, Buono R, Otegui MS. Plant endosomal trafficking pathways. Curr. Opin. Plant Biol. 2011; 14:666–673. [PubMed: 21821464]

Samaj J, Muller J, Beck M, Bohm N, Menzel D. Vesicular trafficking, cytoskeleton and signalling in root hairs and pollen tubes. Trends Plant Sci. 2006; 11:594–600. [PubMed: 17092761]

Schneeberger K, Ossowski S, Lanz C, Juul T, Petersen AH, Nielsen KL, Jorgensen JE, Weigel D, Andersen SU. SHOREmap: simultaneous mapping and mutation identification by deep sequencing. Nat. Methods. 2009; 6:550–551. [PubMed: 19644454]

Spitzer C, Reyes FC, Buono R, Sliwinski MK, Haas TJ, Otegui MS. The ESCRT-related CHMP1A and B proteins mediate multivesicular body sorting of auxin carriers in *Arabidopsis* and are required for plant development. Plant Cell. 2009; 21:749–766. [PubMed: 19304934]

Tanaka H, Kitakura S, De Rycke R, De Groodt R, Friml J. Fluorescence imaging-based screen identifies ARF GEF component of early endosomal trafficking. Curr. Biol. 2009; 19:391–397. [PubMed: 19230664]

Teh OK, Hofius D. Membrane trafficking and autophagy in pathogen-triggered cell death and immunity. J. Exp. Bot. 2014; 65:1297–1312. [PubMed: 24420567]

Wang J, Ding Y, Wang JQ, Hillmer S, Miao Y, Lo S, Wang X, Robinson DG, Jiang L. EXPO, an exocyst-positive organelle distinct from multivesicular endosomes and autophagosomes, mediates cytosol to cell wall exocytosis in *Arabidopsis* and tobacco cells. Plant Cell. 2010; 22:4009–4030. [PubMed: 21193573]

Wesley SV, Helliwell CA, Smith NA, Wang MB, Rouse DT, Liu Q, Gooding PS, Singh SP, Abbott D, Stoutjesdijk PA, Robinson SP, Gleave AP, Green AG, Waterhouse PM. Construct design for efficient, effective and high-throughput gene silencing in plants. Plant J. 2001; 27:581–590. [PubMed: 11576441]

Zhang J, Madden TL. PowerBLAST: a new network BLAST application for interactive or automated sequence analysis and annotation. Genome Res. 1997; 7:649–656. [PubMed: 9199938]

Zhang X, Zhu Y, Liu X, Hong X, Xu Y, Zhu P, Shen Y, Ji Y, Wen X, Zhang C, Zhao Q, Wang Y, Lu J, Guo H. Suppression of endogenous act-siRNA-mediated gene silencing by bidirectional cytoplasmic RNA decay in *Arabidopsis*. Science. 2015; 348:120–123. [PubMed: 25838384]

Zhong S, Fei Z, Chen YR, Zheng Y, Huang M, Vrebalov J, McQuinn R, Gapper N, Liu B, Xiang J, Shao Y, Giovannoni JJ. Single-base resolution methylomes of tomato fruit development reveal epigenome modifications associated with ripening. Nat. Biotechnol. 2013; 31:154–159. [PubMed: 23354102]

Zhuang X, Wang H, Lam SK, Gao C, Wang X, Cai Y, Jiang L. A BAR-domain protein SH3P2, which binds to phosphatidylinositol 3-phosphate and ATG8, regulates autophagosome formation in *Arabidopsis*. Plant Cell. 2013; 25:4596–4615. [PubMed: 24249832]

Zhuang X, Jiang L. Autophagosome biogenesis in plants: roles of SH3P2. Autophagy. 2014; 10:704–705. [PubMed: 24598432]

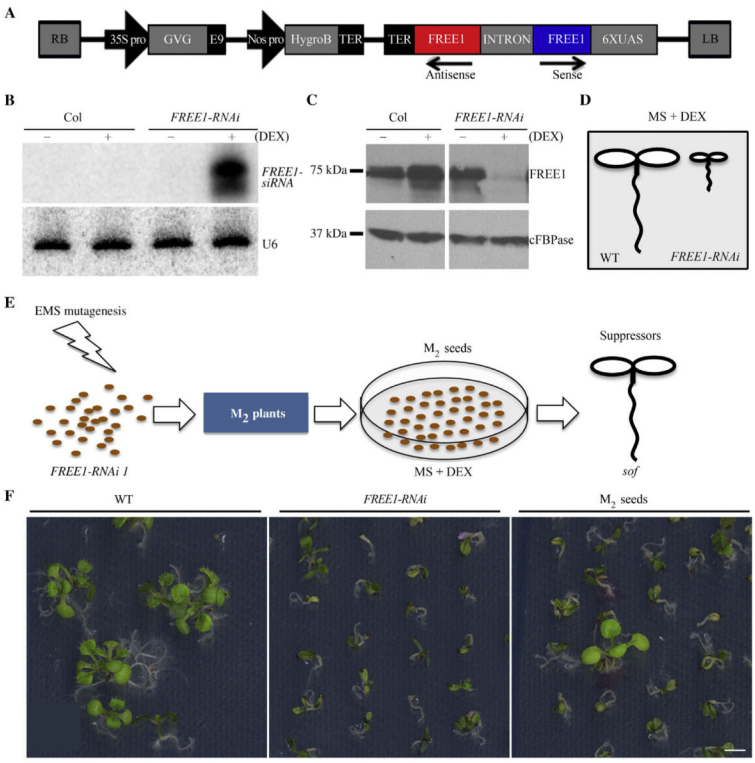

Fig. 1. Illustration of *sof* mutants screening

A: Schematic diagram of the T-DNA constructs in the binary vector pTA7002, which confers hygromycin resistance in plants. **B:** RNA blot analysis with FREE1 probe detected accumulated *FREE1-siRNA* with DEX application in *FREE1-RNAi* line. Detection of U6 served as loading control. **C:** Immunoblot analysis with anti-FREE1 antibody. FREE1 protein level was barely detected in *FREE1-RNAi* plants with DEX treatment. Antibodies against the protein cFBPase served as the loading control. **D:** Diagram showing the seedling lethal phenotype caused by FREE1 loss of function. **E:** Schematic illustration of screening procedure. Single insertion Dex-inducible *FREE1-RNAi* seeds were mutated with EMS, and with DEX induction survived M_2 seedlings were selected as putative *sof* mutants. **F:** Example of primary screening with M_2 seeds plated on MS plates supplied with 10 μmol/L DEX. Scale bar, 5 mm.

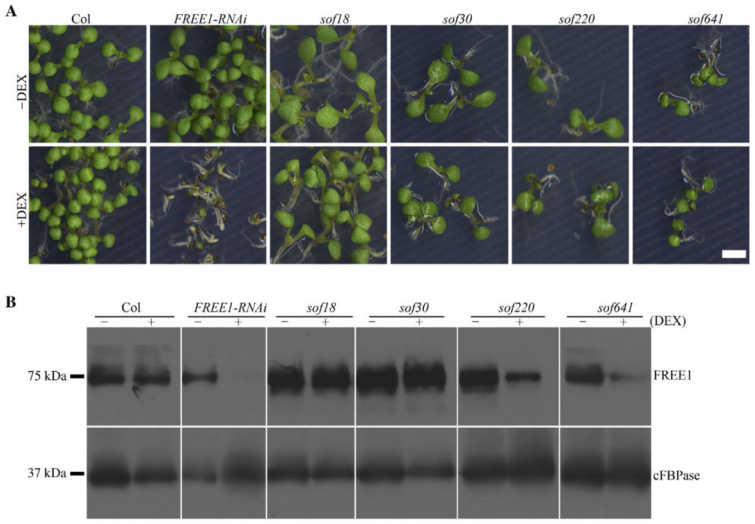

Fig. 2. Representative *sof* mutants characterization with M_3 seeds

A: Seedling survival phenotype of putative *sof* mutants with M_3 seeds plated on MS plates and MS plates supplied with 10 μmol/L DEX. Scale bar, 5 mm. **B:** Immunoblot analysis with anti-FREE1 antibody. FREE1 protein level was not changed in *sof18* and *sof30* with DEX, showing that they are RNAi-related mutants. Reduced FREE1 protein level was detected in *sof220* and *sof641* mutants, showing that they are FREE1-related mutants. Antibodies against the protein cFBPase served as loading control.

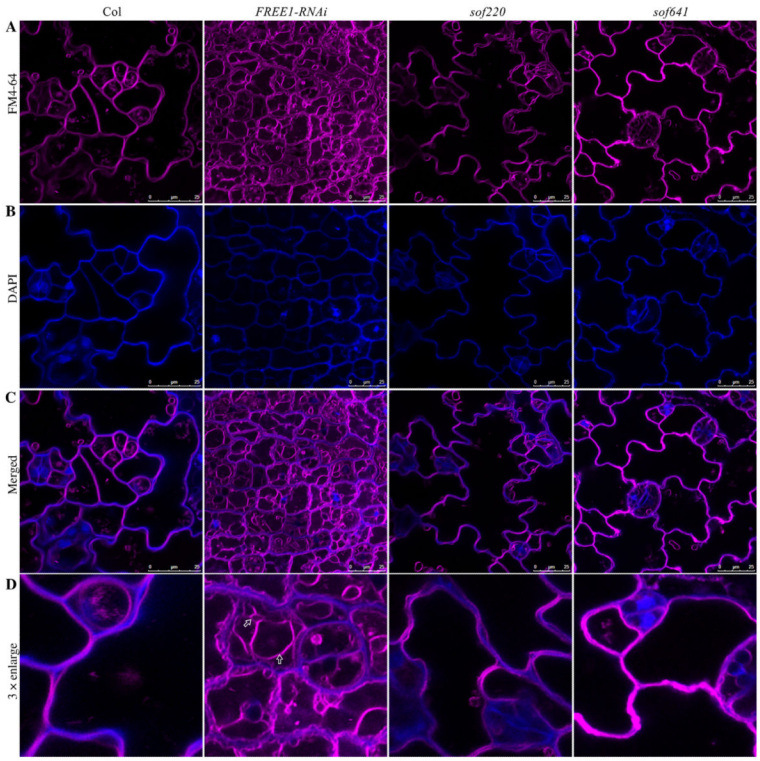

Fig. 3. Vacuole morphology analysis of representative FREE1-related *sof* mutants

A: Vacuole morphology was analyzed using FM 4-64 dye staining. Compared to the wild type plants, fragmented vacuoles were observed in *FREE1-RNAi* plants. FREE1-related *sof* mutants *sof220* and *sof641* showed large central vacuoles. **B:** The short-time DAPI staining was used to visualize the cell shape. **C:** Merged result of FM 4-64 dye staining and DAPI staining. Scale bar, 25 μm. **D:** 3 × enlargement of merged images. Arrows indicated the fragmented vacuoles in *FREE1-RNAi* plants.

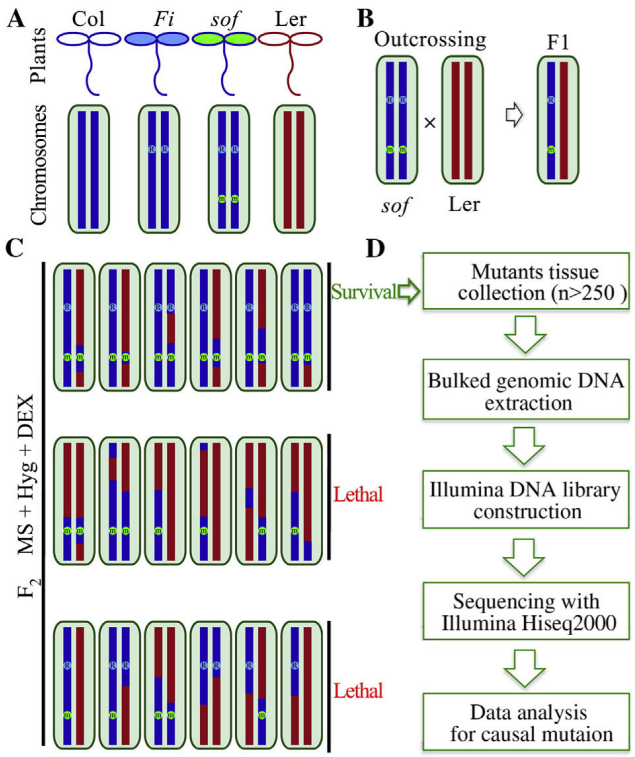

Fig. 4. NGS-mapping workflow

A: The genome of Ler is in red and Col is in blue. From genetic analysis, we know that *FREE1-RNAi* transgenic plants harbor a single-insertion that we marked as R in blue. All *sof* mutants are assumed to harbor a mutation (m in green) caused by EMS. **B:** The putative mutant was first crossed to the Ler wild type. F_1 hybrids inbreeded and gave rise to a segregating F_2 mapping population. **C:** The causal mutation was identified using segregating populations from F_2 *via* outcrossing with Ler ecotype wild type. Survived seedlings from F_2 Seeds were pooled together for genomic DNA on medium containing both hygromycin antibiotics and DEX. In the case of recessive *sof* mutations, this will include only homozygous mutants, which should be around 3/16 of all seeds. **D:** Illumina sequencing library was constructed using obtained bulked DNA. Whole genome sequencing was performed using Hiseq2000 platform. Further sequencing data analysis would uncover the causal mutation.

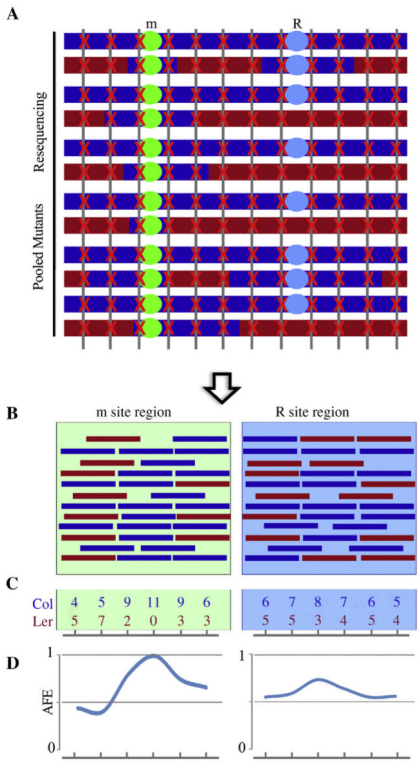

Fig. 5. Analysis strategy and simulative results for mapping-by-sequencing

A: Schematic of mapping mutants and whole genome sequencing. The m site was selected during the mapping sample pooling process. They are colored after the parental genomes from which they were sampled. The red cross marks reads hit along with the genome. **B:** Simulative reads aligned to m site region and R site region. Reads in red stand for Ler genome and reads in blue stand for Col genome. **C:** Examples of reads counts from simulate reads alignment to parental genomes. **D:** Allele frequency estimations of both m site region and R site region. One Col allele frequency peak should correspond to the causal m site region, while a mild Col allele frequency peak may appear at R site region.

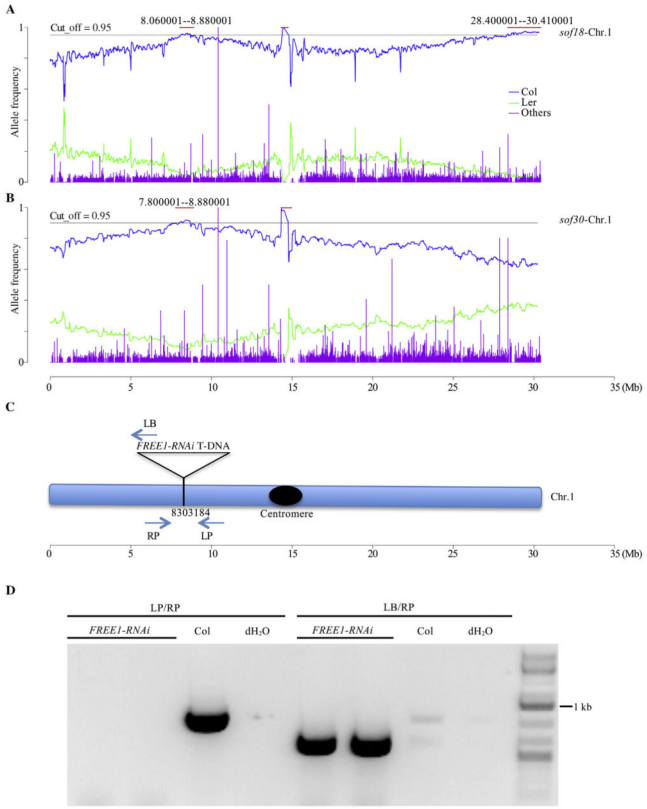

Fig. 6. Sequencing results of *sof18 & sof30* identified the *FREE1-RNAi* T-DNA insertion site

A: Allele frequency analysis result of *sof18* on chromosome 1. Two Col-allele peaks located on chromosome 1, the peak appeared in the middle region due to centromere, and the far right peak is specific to *sof18*. **B:** Allele frequency analysis result of *sof30* chromosome 1. One Col-allele peak located on chromosome 1, and shared by *sof18* with the left peak. **C:** Shared peak on chromosome 1 between *sof18* and *sof30* corresponded to the R site (*FREE1-RNAi* T-DNA insertion site), which was the insertion site of *FREE1-RNAi* T-DNA. **D:** Genomic DNA PCR confirmed the *FREE1-RNAi* T-DNA insertion site.

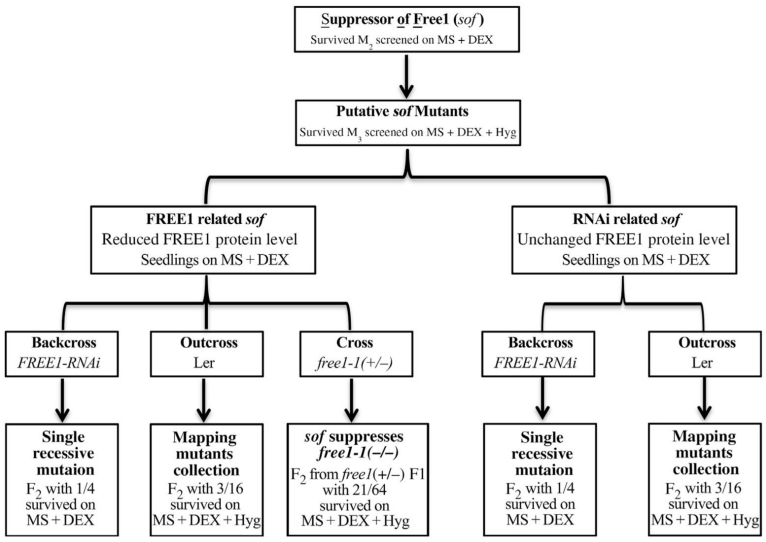

Fig. 7. Flowchart summarizing the whole process of screening

To further uncover the functional mechanism of FREE1, suppressors of *free1* (*sof* for short) were screened using EMS-treated M_2 seeds of a single insertion Dexinducible *FREE1-RNAi* line. Putative M_3 seeds were classified into FREE1-related and RNAi-related groups through FREE1 protein level detection. Mutants with reduced FREE1 protein level were termed as FREE1-related *sof* mutants while those with no changes in FREE1 protein levels were termed RNAi-related *sof* mutants. For both FREE1-related and RNAi-related *sof* mutants, a backcross with *FREE1-RNAi* line was used to detect whether the mutation was a single recessive mutation. To map the mutated gene, outcrossing with Ler was used to establish the mapping mutants pool for both FREE1-related and RNAi-related *sof* mutants. For FREE1-related *sof* mutants, a cross with *free1-1* T-DNA knockout line was used to verify that the *sof* mutation was able to suppress the lethal phenotype of *free1-1*.

Table 1

Summary of *sof* screening.

Generation	Number
M_1	10,000
M_2	1500 from ~40,000
M_3	84 FREE1-related
M_3	145 RNAi-related

For *sof* screening, 10,000 *FREE1-RNAi* M_0 seeds were mutagenized with EMS, and 1500 *sof* mutants were screened out from about 40,000 M_2 seeds. In total, about 230 mutants were identified for restoring the lethality phenotype in M_3 generation. Western blot analysis using anti-FREE1 antibody with M_3 generation plants further identified 84 FREE1-related suppressor mutants and 145 RNAi-related mutants.